Deep Learning–Based Multiclass Classification of Mitral Valve Etiologies Using Limited B-Mode and Color Doppler Echocardiography: Internal and External Validation

Dawun Jeong, BS[a†], Moon-Seung Soh, MD[b†], Jaeik Jeon, MS[c], Hyunseok Jeong, PhD[a], JunHeum Cho, MS[c], Jiyeon Kim, MS[c], Jina Lee, PhD[d], Seung-Ah Lee, MD, PhD[c], Joon-Han Shin, MD[b], Yeonggul Jang, PhD[c]*, Yeonyee E. Yoon, MD, PhD[c,e]*, Hyuk-Jae Chang, MD, PhD[c,f]

[a]Department of Internal Medicine, Graduate School of Medical Science, Brain Korea 21 Project, Yonsei University College of Medicine, Seoul, Republic of Korea

[b]Department of Cardiology, Ajou University School of Medicine, Suwon-si, Gyeonggi-do, Republic of Korea

[c]Ontact Health Co., Ltd., Seoul, Republic of Korea

[d]Yonsei University Health System, Seoul, Republic of Korea

[e]Cardiovascular Center and Division of Cardiology, Department of Internal Medicine, Seoul National University Bundang Hospital, Seongnam, Gyeonggi, Republic of Korea

Department of Internal Medicine, Seoul National University College of Medicine, Seoul, Republic of Korea

[f]Division of Cardiology, Severance Cardiovascular Hospital, Yonsei University College of Medicine, Yonsei University Health System, Seoul, Republic of Korea

†The first two authors contributed equally to this work.

Running Title: DL for Multiclass Mitral Valve Disease

Word count: 4,304

***Corresponding authors:**

Yeonyee E. Yoon, MD, PhD

Professor, Division of Cardiology, Cardiovascular Center

Seoul National University Bundang Hospital

82, 173 Beon-gil, Gumi-ro, Bundang-gu, Seongnam-si, Gyeonggi-do, Republic of Korea

Phone: 82-31-787-7072

Email: yeonyeeyoon@snubh.org

And

Yeonggul Jang, PhD

Ontact Health Co., Ltd., Seoul, Republic of Korea

50-5, Ewhayeodae-gil, Seodaemun-gu, Seoul, Republic of Korea

Phone: 82-2-362-9610

E-mail: ygjang@ontacthealth.com

ABSTRACT

Background: Accurate etiologic classification of mitral valve (MV) is essential for guiding clinical management but remains dependent on expert visual interpretation. Despite advances in artificial intelligence (AI)-based quantitative analysis, automated morphologic interpretation under routine imaging conditions remains limited.

Objectives: To develop and validate a deep learning (DL) framework for multiclass classification for major MV etiologies using a limited routine transthoracic echocardiography (TTE) view.

Methods: A multi-view DL model was developed to classify five MV etiologies (normal, rheumatic, degenerative, prolapse, and functional). The developmental dataset comprised 4,344 TTE examinations from a nationwide multicenter registry. Validation was performed using an internal test dataset and an independent external test dataset (2,262 TTE examinations). Prespecified subgroup analyses were conducted according to mitral regurgitation (MR) severity and automated image quality (IQ).

Results: The model demonstrated robust performance across all MV etiologies in both internal and external datasets. In the internal test dataset, area under the receiver operating characteristic curve (AUROC) values ranged from 0.968 to 0.997 across etiologies, with higher performance observed for normal valves and rheumatic disease. In the external test dataset, discriminative performance remained preserved (AUROC, 0.931-0.992), despite differences in disease distribution and MR severity. Sensitivity for MV prolapse increased markedly with moderate-to-severe MR compared with mild MR, whereas degenerative disease showed persistently lower sensitivity across MR severity. Diagnostic performance remained stable across IQ strata, with comparable accuracy and macro-F1 scores in all-adequate and partially suboptimal

examinations. In post-hoc analyses of cases with multiple MV etiologies, the model correctly identified at least one expert-assigned etiology in 85.7% of cases.

Conclusions: DL-based analysis of limited, routinely acquired TTE views enables reliable multiclass classification of MV etiologies. This approach may complement quantitative automation and expert visual assessment, supporting more consistent and scalable MV evaluation in routine echocardiographic practice.

Keywords: Mitral Valve Disease, Etiology Classification, Echocardiography, Deep Learning, Multiclass Classification

1. INTRODUCTION

Echocardiography is the primary imaging modality for evaluating valvular heart disease (VHD). Comprehensive echocardiographic assessment of VHD requires both morphological and functional evaluation of the affected valve.[1,2] Quantitative hemodynamic measurements, such as Doppler-derived transvalvular gradients and flow parameters, play a central role in determining functional severity and have already been standardized to a large extent.[1,2] In contrast, the assessment of morphological abnormalities that underlie valvular dysfunction still relies heavily on expert visual interpretation. This process is inherently operator-dependent, experience-driven, and therefore less reproducible across readers and institutions.

Artificial intelligence (AI)-based interpretation of echocardiography has rapidly expanded in recent years.[3,4] Initial efforts mainly focused on automating quantitative measurements, and many manual parameters can now be reliably extracted by AI.[4-8] These advances have also been applied to VHD, where AI can automate key components of diagnosis and grading.[6,9-11] However, the evaluation of valvular morphology remains largely dependent on human expertise. This challenge is particularly pronounced for the mitral valve (MV), where comprehensive assessment requires detailed evaluation of not only the leaflets but also the subvalvular apparatus. Moreover, determining the underlying etiology of MV disease is essential for guiding management decisions,[1,2] yet accurate classification is difficult outside specialized centers. These limitations underscore the need for AI systems capable of consistently providing expert-level morphological interpretation.

Therefore, we sought to develop a deep learning (DL) model capable of MV etiology classification using limited B-mode and color Doppler echocardiographic inputs. The model was designed to differentiate normal valves from four major etiologic categories of MV disease

– rheumatic, degenerative, prolapse, and functional – encompassing both mitral stenosis (MS) and mitral regurgitation (MR). We further aimed to rigorously evaluate model performance using internal and external test datasets from independent cohorts to assess its generalizability and clinical applicability.

2. MATERIAL AND METHODS

2.1. Study Population

In this study, the DL framework was developed using data from the Open AI Dataset Project (AI-Hub), a nationwide echocardiography repository funded by the Ministry of Science and ICT of the Republic of Korea.[12] The database includes approximately 30,000 transthoracic echocardiographic (TTE) examinations, obtained retrospectively from several tertiary medical centers across South Korea between 2012 and 2021, representing a diverse range of cardiovascular pathologies.[6-8,13] For model development, a total of 4,344 TTE examinations from 4,317 patients were used, comprising both cases with MV pathology and individuals without MV disease. Normal controls were identified from the "normal" category of the database and consisted of asymptomatic individuals who underwent TTE examinations as a part of routine health evaluation. Only examinations demonstrating entirely normal MV structure and function were included in the control group. Cases with MV disease were obtained from the "MV disease" category and identified using ICD-10 diagnostic codes I05.0, I05.1, I34.0, and I34.2. TTE examinations demonstrating the presence of MS or MR of at least mild severity were included, whereas studies confirming normal MV function were excluded.[1,2,14] Examinations in which the assessment of the native MV was not feasible were excluded. These included cases with any prosthetic heart valve, prior MV surgery or intervention (including percutaneous mitral valvotomy), tricuspid annuloplasty, ascending aorta replacement, or complex congenital heart disease, were excluded. In contrast, procedures that do not directly affect the native MV, such as pacemaker or cardioverter-defibrillator implantation, cardiac resynchronization therapy, simple atrial or ventricular septal defect repair, coronary artery bypass grafting, or abdominal aorta aneurysm repair, were not considered exclusion criteria. All eligible examinations were subsequently categorized by underlying MV

etiology. Cases with multiple MV disease etiologies were excluded from the developmental dataset. The final developmental dataset consisted of 1,391 normal studies, 469 rheumatic cases, 162 degenerative cases, 1,478 prolapse cases, and 844 functional cases. This cohort was then randomly divided into training, validation, and internal test subsets in an 8:1:1 ratio, yielding 3,458 patients in the training set, 429 in the validation set, and 430 in the internal test set, corresponding to 3,485, 429, and 430 TTE examinations, respectively. (**Table 1**) To avoid data leakage, all TTE examinations from patients who underwent multiple TTE studies were assigned exclusively to the training set. In contrast, patients included in the validation and internal test set each contributed a single TTE examination.

An external test cohort was additionally assembled using 2,254 TTE examinations from 2,262 patients obtained at Ajou University Hospital between 2020 and 2024. Normal controls in this cohort were randomly selected from subjects whose studies were reviewed and confirmed to demonstrate normal MV morphology and function. Cases representing a broad spectrum of MV etiologies were included to ensure comprehensive evaluation of model performance. The external dataset comprised the following etiologic categories: normal (n=542), rheumatic (n=269), degenerative (n=507), prolapse (n=308), and functional (n=636). The institutional review boards of all participating hospitals approved the study protocols and waived the requirement for informed consent owing to the retrospective and observational study design (2021-0147-003 / CNUH 2021-04-032 / HYUH 2021-03-026-003 / SCHBC 2021-03-007-001 / B 2104/677-004). Additional approval for the construction and use of the external test cohort was obtained from the IRB of Ajou University Hospital (AJOUIRB-DB-2024-430). All clinical and echocardiographic data were fully anonymized prior to analysis.-

2.2. TTE Acquisition and Utilization

All TTE examinations were performed by trained sonographers or cardiologists and were initially interpreted by board-certified cardiologists specializing in echocardiography, following current clinical practice guidelines.[1,2,15] To ensure accurate labeling of the developmental dataset, two expert cardiologists (S.A. Lee, > 10 years of experience; Y.E. Yoon, > 15 years of experience) independently reviewed the complete TTE studies for each case. Any discrepancies were resolved through consensus, and final diagnostic labels were assigned accordingly. Importantly, although expert annotations were derived from a comprehensive review of the entire TTE examination, only a limited set of standard views was used as input to the DL framework. The selected views included the parasternal long-axis (PLAX) and apical four-chamber (A4C) views, with and without color Doppler. Because the present framework was designed to classify a single dominant etiology of MV pathology, cases with overlapping morphological features (e.g., degenerative changes with superimposed functional regurgitation) were excluded from the developmental dataset. These cases were retained separately and used for additional analyses to further assess model robustness. For the external test dataset, labeling procedures were designed to reflect real-world clinical practice. The etiologies of MV pathology were primarily determined from the original TTE reports generated at the contributing institution. All cases in the external test dataset were assigned a single predominant MV etiology, which was independently reviewed and confirmed by an experienced cardiologist (M.S. Soh, > 5 years of experience) who was not involved in labeling the development dataset.

To preserve real-world clinical variability, both the developmental and external test datasets included all available TTE examinations without exclusion based on image quality (IQ) or examination completeness. Examinations were retained even when only the PLAX view was available, as well as when specific target views were missing, or image quality was suboptimal.

When multiple video clips were available for a given TTE view, all clips were provided to the DL-based model as input. Conversely, the absence of any individual view did not preclude inclusion of the examination. IQ was assessed using an automated, model-based approach rather than subjective human visual grading.

2.3. DL-Based Framework

To select the target TTE views and assess IQ, we applied our previously developed AI-based automatic TTE analysis system (Sonix Health; Ontact Health Co., Ltd, Korea).[5-8,16] Target views included the PLAX view, a PLAX view with zoomed visualization of the MV, both acquired with and without color Doppler, and the A4C view with and without color Doppler. Automated identification of these target views was performed using the system's view classification module. The investigators then reviewed all selected clips to remove misclassified views and recover any missing ones, thereby ensuring consistent and accurate inputs for the DL model. Following view selection, the IQ of the retained video clips was evaluated using the system's segmentation module.[5-8,16] IQ was quantified from the entropy of the segmentation outputs and categorized into four levels (good, fair, poor, and non-diagnostic). Detailed descriptions of the segmentation-based IQ assessment are provided in **Supplemental Methods 1**.

Building upon the selected TTE views, we developed a multi-view DL architecture for MV disease etiology classification, designed to reflect the established clinical assessment workflow. The proposed architecture consists of three key components: (1) a shared MViT-Small encoder[17] that extracts unified spatiotemporal representations across all input views; (2) view-specific projection heads that disentangle and process anatomical features while

accommodating missing views via learnable embeddings; and (3) a learnable gating mechanism that dynamically refines valve-related features by integrating zoomed morphological details when available. (**Figure 1**)

A shared spatiotemporal encoder based on MViT-Small was used to extract a unified video representation for all TTE views. The shared encoder enabled consistent feature learning while accommodating variable view availability across examinations. To handle missing views efficiently, only available views were processed via batch-wise concatenation, rather than by zero-padding absent inputs. The MViT-Small encoder, which incorporates multi-scale attention mechanisms, was initialized with weights pretrained on an in-house TTE view classification task to leverage domain-specific representations. For each input view, the encoder generated a fixed-length feature embedding, which was subsequently used for downstream MV etiology classification. Detailed input dimensions, batch-wise concatenation procedures, and view-specific feature separation are provided in **Supplementary Methods 2**.

To reflect established clinical interpretation workflows, encoder features from each view were processed through view-specific projection modules. Features derived from the PLAX view were decomposed into valve-specific and cavity-related representations, mirroring the clinical practice of separately assessing valvular morphology and ventricular context in this view. In contrast, the A4C and color Doppler views are typically interpreted by evaluating overall chamber geometry and flow dynamics as integrated information rather than isolating valve and cavity components. Accordingly, features from these views were projected into a shared representation space without further decomposition into valve and cavity components, allowing them to contribute complementary chamber-level and hemodynamic information that is less accessible from the PLAX perspective. PLAX-zoomed views were not directly used for classification; instead, they were incorporated to refine valve-specific representations through

a learnable, zoom-aware gating mechanism. This mechanism dynamically integrated detailed zoomed morphological information when available, while defaulting to standard PLAX-derived valve features when zoomed views were absent. Additional methodological details are available in **Supplementary Methods 3.**

Final MV etiology classification was performed by integrating information from all available TTE views. The refined valve representation, cavity-related features from the PLAX view, and complementary features from the apical four-chamber and color Doppler views were concatenated to form a unified feature representation. Missing views were handled using learnable embeddings to ensure robustness to variable view availability. The fused representation was then passed to a linear classification head to predict one of five etiologic categories (normal, prolapse, rheumatic, functional, or degenerative mitral valve disease). The model was trained using a composite objective function that combined classification loss with auxiliary regularization terms to promote stable feature learning and effective use of zoomed morphological information. Detailed descriptions are provided in **Supplemental Method 4.**

The model was trained using the AdamW optimizer with learning rate scheduling and regularization strategies to promote stable convergence and prevent overfitting. The checkpoint achieving the best performance on the validation set was selected for final evaluation. Detailed training configurations are provided in **Supplementary Methods 5**.

2.4. Validation and Statistical Analysis

Model performance was evaluated using standard classification metrics, including overall accuracy, balanced accuracy, and macro-F1 score as global performance metrics. In addition, class-specific diagnostic performance was assessed for each MV etiology using accuracy,

precision, sensitivity, specificity, F1-score, and the area under the receiver operating characteristic curve (AUROC). Class-wise accuracy, precision, sensitivity, specificity, and F1-score were derived from confusion matrices using counts of true positives, true negatives, false positives, and false negatives. AUROC was calculated for each etiology using a one-vs-rest strategy, with receiver operating characteristic curves generated by varying classification thresholds based on predicted class probabilities.

To further investigate factors potentially contributing to performance differences between datasets, additional stratified analyses were performed in cases with at least mild MR. Specifically, model performance was evaluated separately in mild MR and moderate-to-severe MR subgroups. In addition, IQ-stratified analyses were also conducted to assess model robustness under variable imaging conditions. Automated IQ assessment was applied to B-mode TTE views (PLAX, PLAX zoomed MV, and A4C). Based on these assessments, examinations were categorized into an all-adequate group, in which all input views met at least fair IQ, and a partially suboptimal group, in which one or more input views were rated below the fair threshold. Model performance was compared between these groups using the same diagnostic metrics described above.

To qualitatively assess model interpretability, attention-based visualization was performed using self-attention weights extracted from the final layer of the MViT encoder. Attention maps were generated to identify spatiotemporal regions prioritized by the model during feature extraction. This approach was selected in preference to gradient-based visualization methods due to architectural constraints related to global pooling and multi-view feature fusion. Attention weights were averaged across heads and frames and overlaid on representative echocardiographic images to visualize anatomically relevant focus areas, such as valve leaflets and surrounding structures.

3. RESULTS

3.1. Baseline Characteristics of the Study Population

Baseline Characteristics and the distribution of MV pathology across datasets are shown in **Table 1.** Within the developmental dataset, the training, validation, and internal test subsets were well balanced with respect to age, sex, body mass index, prevalence of MS and MR, and MV etiology (all $p > 0.05$). Compared with the internal test dataset, patients in the external test dataset were older and had a higher prevalence of both MS and MR. In addition, the distribution of MV etiologies differed significantly between the internal and external test datasets ($p < 0.001$), with the external dataset showing a higher proportion of degenerative and functional etiologies and a lower proportion of prolapse. Furthermore, the severity distribution of MR differed between the developmental and external datasets, with the external cohort demonstrating a higher proportion of mild MR and a lower proportion of severe MR across multiple MV etiologies (**Figure 2**). In contrast, differences in MS severity distribution between datasets were less pronounced (**Supplementary Results 1**).

3.2. Diagnostic Performance of the DL Model in Internal and External Datasets

In the internal test dataset (n=430), the model achieved an overall accuracy of 0.916, a balanced accuracy of 0.867, and a macro-F1 score of 0.857, indicating robust and well-balanced classification performance across etiological categories. In the external test dataset (n=2,262), overall performance remained high, with an overall accuracy of 0.813, a balanced accuracy of 0.792, and a macro-F1 score of 0.804, supporting the generalizability of the model across independent cohorts. The diagnostic performance of the proposed DL model for MV etiology classification is summarized using confusion matrices (**Figure 3)** and detailed quantitative

performance metrics (**Table 2**).

In the internal test dataset, excellent performance for normal valves was observed, with an accuracy of 0.986, a sensitivity of 0.993, and an AUROC of 0.997. High diagnostic performance was also observed for rheumatic disease (accuracy 0.970, AUROC 0.968) and degenerative disease (accuracy 0.981, AUROC 0.980), although degenerative cases showed relatively lower sensitivity compared with other etiologies. For prolapse, the model demonstrated high accuracy (0.951) and AUROC (0.985), with balanced precision and sensitivity. Functional MV disease was classified with an accuracy of 0.944 and an AUROC of 0.969, showing slightly lower sensitivity compared with normal valves but preserved overall discriminative performance.

In the external test dataset, overall diagnostic performance remained high, supporting the model's generalizability across independent cohorts. Classification of normal valves remained robust, with an accuracy of 0.938 and an AUROC of 0.992. For rheumatic disease, the model maintained strong performance, achieving an accuracy of 0.966 and an AUROC of 0.966. Degenerative MV disease demonstrated slightly lower accuracy (0.885) but preserved discriminative ability (AUROC = 0.931), although sensitivity was reduced compared with other etiologies (0.600). Prolapse also showed a modest decline in sensitivity (0.662) in the external dataset, with an accuracy of 0.942 and an AUROC of 0.942. Functional MV disease demonstrated high sensitivity (0.910) and an AUROC of 0.957, indicating robust discriminative performance despite modestly reduced accuracy (0.895), comparable to that observed for degenerative disease. Confusion matrix analysis revealed that most misclassifications occurred between prolapse, degenerative, and functional etiologies, reflecting overlapping morphological and hemodynamic features among these categories, whereas normal and rheumatic etiologies were more consistently classified across both datasets.

Given the observed differences in diagnostic performance between the internal and external test datasets, additional analyses were performed to assess the potential impact of MR severity distribution. When cases were stratified by MR severity, overall model performance improved in the moderate-to-severe MR subgroup, with higher overall accuracy (0.856 vs. 0.676), balanced accuracy (0.582 vs. 0.512), and macro-F1 score (0.593 vs. 0.546) compared with mild MR cases. At the etiologic level, the diagnostic performance for prolapse improved substantially when the analysis was restricted to moderate-to-severe MR, with a corresponding increase in sensitivity compared with mild MR cases (0.837 vs. 0.330). In contrast, sensitivity for degenerative MV disease did not show a comparable improvement after severity stratification (0.355 vs. 0.601). Detailed results of the severity-stratified analyses are presented in **Supplemental Results 2**.

3.3. Performance in Cases with Multiple MV Pathologies

Although cases with multiple coexisting MV disease etiologies were excluded from the developmental dataset because a single dominant etiology could not be clearly determined, we performed a post-hoc inference analysis to examine model behavior in this clinically relevant subgroup. A total of 63 such cases were identified and analyzed. The most common mixed-etiology pattern was combined functional and degenerative MV disease, accounting for 18 of 63 cases; the detailed distribution of mixed etiologies is provided in **Supplementary Results 3**. Among all mixed-etiology cases, the DL model correctly predicted the expert-designated primary etiology in 42 cases (66.7%). In an additional 12 cases (19.0%), the model prediction corresponded to the secondary (comorbid) etiology identified by expert reviewers. Overall, the model predicted one of the expert-recognized etiologies in 54 of 63 cases (85.7%), despite not being trained using mixed-etiology labels. (**Supplementary Results 3**) The remaining 9 cases

were misclassified into etiologic categories not identified by expert review. These cases typically demonstrate complex or overlapping morphological and hemodynamic features, highlighting the inherent ambiguity in assigning a single dominant etiology in advanced or mixed MV disease. Representative examples of model predictions in mixed-etiology cases are illustrated in **Figure 4**.

3.4. Subgroup Analyses According to Image Quality

Model performance was further evaluated using IQ to assess robustness under varying image conditions. When examinations were stratified into all-adequate and partially suboptimal groups, overall diagnostic performance remained largely preserved across both internal and external test datasets. (**Supplemental Results 4**) In the internal test dataset, overall accuracy, balanced accuracy, and macro-F1 score were comparable between the two IQ subgroups (0.932 vs. 0.883; 0.853 vs. 0.879; and 0.849 vs. 0.859, respectively), with no systematic degradation in class-wise performance observed in the partially suboptimal group. Consistent findings were observed in the external test dataset. Overall accuracy, balanced accuracy, and macro–F1 score were similar between the all-adequate and partially suboptimal groups (0.808 vs. 0.825; 0.776 vs. 0.829; and 0.791 vs. 0.823, respectively), indicating that incomplete or partially suboptimal IQ did not result in a clinically meaningful decline in model performance. Across etiologic categories, sensitivity and AUROC values remained broadly comparable across image quality strata, supporting the robustness of the proposed model in real-world imaging conditions in which optimal view acquisition may not always be feasible.

3.5. Attention Map-Based Model Interpretability Analysis

Attention map analysis was conducted to qualitatively assess whether the model focused on anatomically relevant regions during feature extraction. Representative cases containing all five target views were selected for each MV etiology category. As shown in **Figure 5**, the model predominantly attended to the MV apparatus across all categories and views, including normal valves. In PLAX and PLAX-zoomed views, attention was predominantly concentrated on the MV leaflet and annular regions. In A4C views, attention remained largely focused on the MV apparatus. In color Doppler views, attention extended beyond valvular anatomy to include regions corresponding to regurgitant flow in cases with MR. These attention patterns were consistently observed across prolapse, rheumatic, functional, and degenerative MV etiologies. Overall, the attention maps suggest that the model prioritizes anatomically and physiologically relevant regions when extracting features for MV etiology classification.

4. DISCUSSIONS

In this study, we developed a DL-based framework for the classification of normal and four major MV disease etiologies using a limited set of routinely acquired B-mode and color Doppler TTE views. The model demonstrated stable and reproducible performance in both internal and external test cohorts, supporting its generalizability across independent clinical settings. Diagnostic performance was particularly high for normal valves and rheumatic MV disease, while overall accuracy and discriminative ability were largely preserved in the external cohort despite differences in disease severity distribution. Importantly, model performance remained robust across analyses stratified by MR severity, IQ, and the presence of mixed MV pathologies. Together, these findings suggest the feasibility of inferring MV etiology from limited echocardiographic inputs under routine clinical imaging conditions.

AI-based echocardiographic analysis has rapidly evolved in recent years. Early applications primarily focused on automating quantitative measurements[5-8,18,19], whereas more recent approaches have expanded toward replicating expert visual interpretation.[20,21] These advances have been applied to VHD, initially automating diagnosis and severity grading based on quantitative parameters, most notably for aortic stenosis,[6,22,23] and subsequently by directly analyzing echocardiographic videos to detect VHD and estimate severity, either through valve-specific algorithms[6,11,24-26] or as part of a full-examination framework.[27,28] Despite recent advances in AI-based echocardiographic analysis, automated interpretation of valvular morphology, particularly for etiologic classification, remains challenging. This limitation is most evident in MV disease, where accurate etiologic assessment requires integration of leaflet and subvalvular features and has direct implications for clinical management. In this context, we developed and validated a DL-based framework designed to infer MV etiology from B-mode and color Doppler inputs under routine clinical imaging conditions.

In the present study, etiology-specific analyses provided insight into the observed performance patterns. Diagnostic separability was highest for normal valves and rheumatic MV disease, reflecting their relatively distinct morphological features. In contrast, performance varied among non-rheumatic MR etiologies and was differentially influenced by disease severity. Sensitivity for MV prolapse improved in moderate-to-severe MR, consistent with amplification of characteristic morphological features, whereas degenerative MV disease showed limited severity-dependent improvement, likely due to intrinsic heterogeneity and overlap with prolapse and functional MR. In the external test cohort, modest performance attenuation among non-rheumatic MR etiologies may also reflect single-etiology labeling despite frequent morphological overlap in routine practice. Post-hoc analyses of mixed-etiology cases further support a continuum among non-rheumatic MR etiologies, as the model frequently identified either the primary or secondary expert-assigned etiology. Collectively, these findings suggest that the DL model captures latent etiologic structure within echocardiographic morphology, with performance modulated by disease severity and phenotypic overlap.

The proposed framework demonstrated stable diagnostic performance across varying IQ conditions, with no clinically meaningful degradation observed in examinations with partially suboptimal views. This robustness likely reflects the model design, which explicitly accommodates incomplete or lower-quality inputs through multi-view feature integration and learnable representations for missing views. Importantly, IQ was assessed using an automated, model-based approach rather than subjective visual grading, enhancing objectivity and reproducibility. These findings are clinically relevant, as real-world TTE acquisition is frequently constrained by patient-related factors and variable examination conditions. The preserved performance under suboptimal IQ supports the feasibility of applying the proposed

model in routine clinical workflows, where optimal visualization of all target views cannot be consistently guaranteed.

The ability to infer MV etiology from limited, routinely acquired TTE views has several potential clinical implications. In routine, accurate etiologic assessment of MV disease often depends on operator expertise and may be challenging outside specialized centers. An AI-based framework capable of providing consistent etiologic suggestions could support early diagnostic triage and structured reporting, particularly in high-volume or resource-limited settings. By differentiating among major MV disease etiologies, the proposed model may assist clinicians in identifying cases that warrant further expert review or advanced imaging, rather than replacing comprehensive echocardiographic interpretation. In addition, automated etiologic classification could complement existing AI tools focused on quantitative measurement and severity grading, contributing to more standardized and reproducible MV assessment. Collectively, these findings suggest that DL-based etiologic analysis may serve as a supportive component within AI-augmented echocardiographic workflows.

Several limitations of this study should be acknowledged. First, the proposed framework was developed under the assumption of a single dominant MV etiology, whereas mixed or overlapping pathologies are common in clinical practice. Although post-hoc analyses suggested that the model captures overlapping etiologic features, performance in such cases remains inherently constrained by single-label training and evaluation. Second, etiologic classification was performed using a limited set of standard echocardiographic views rather than the full transthoracic echocardiographic examination. While this design choice reflects routine clinical acquisition and enhances feasibility, a comprehensive etiologic assessment may benefit from integrating additional views and complementary quantitative information. Building on experience with the current framework, we are developing an advanced model to

analyze the full echocardiographic examination by integrating vision-based interpretation and quantitative measurements. Third, external validation relied on real-world clinical labels assigning a single predominant etiology, which may have contributed to performance attenuation for non-rheumatic MR etiologies characterized by substantial morphological overlap. Finally, although attention-based visualization provided qualitative insight into model behavior, it does not establish causal relationships between specific imaging features and model predictions and should be interpreted as an explanatory aid rather than definitive evidence of feature importance.

5. CONCLUSIONS

In this study, we demonstrated that DL–based analysis of limited, routinely acquired B-mode and color Doppler TTE views can support etiologic classification of MV disease. The proposed framework achieved stable performance across internal and external cohorts and remained robust under variations in disease severity, image quality, and etiologic overlap. These findings suggest that AI-based morphologic interpretation may complement quantitative automation and expert visual assessment, thereby providing a scalable approach to evaluating MV etiology in routine echocardiographic practice.

Contributors

Dawun Jeong: Data Curation, Methodology, Formal Analysis

Moon-Seung Soh: Validation, Investigation, Data Curation, Echocardiographic review, and annotation

Jaeik Jeon: Software, Methodology, Resources

Hyunseok Jeong: Data Curation, Methodology

JunHeum Cho: Software, Methodology, Resources

Jiyeon Kim: Software, Methodology, Resources

Jina Lee: Data Curation, Methodology

Seung-Ah Lee: Investigation, Supervision, Echocardiographic review, and annotation

Yeonggul Jang: Software supervision, Technological methodology oversight

Yeonyee E. Yoon: Conceptualization, Supervision, Echocardiographic review and annotation, Clinical interpretation, Writing, Review, and Editing

Hyuk-Jae Chang: Conceptualization, Supervision, Funding acquisition

All authors read and approved the final version of the manuscript.

Acknowledgments

This work was supported by a grant from the Institute of Information & Communications Technology Planning & Evaluation (IITP) funded by the Korean government (Ministry of Science and ICT) (No.2022000972, Development of a Flexible Mobile Healthcare Software Platform Using 5G MEC); and the Medical AI Clinic Program through the NIPA funded by the MSIT. (Grant No.: H0904-24-1002).

Declaration of Interests

J.J., J Cho, J Kim, S.A.L., Y.J., and Y.E.Y. are currently affiliated with Ontact Health Co., Ltd. Y.E.Y., and H.J.C. hold stock in Ontact Health Co., Ltd. The other authors have no conflicts of interest to declare.

Data Sharing Statement

The AI-Hub dataset used in this study may be available upon proper request and approval of a formal proposal. The external test dataset cannot be made publicly shared due to ethical restrictions imposed by the IRB of the study institution, as public access could compromise patient confidentiality and privacy. Researchers interested in accessing the minimal anonymized dataset may contact the corresponding author (yeonyeeyoon@gmail.com) for further information.

REFERENCES

[1] Members WC, Otto CM, Nishimura RA, et al. 2020 ACC/AHA guideline for the management of patients with valvular heart disease: a report of the American College of Cardiology/American Heart Association Joint Committee on Clinical Practice Guidelines. Journal of the American College of Cardiology. 2021;77:e25-e197.

[2] Vahanian A, Beyersdorf F, Praz F, et al. 2021 ESC/EACTS Guidelines for the management of valvular heart disease: Developed by the Task Force for the management of valvular heart disease of the European Society of Cardiology (ESC) and the European Association for Cardio-Thoracic Surgery (EACTS). Eur Heart J. 2022;43:561-632.

[3] Davis A, Billick K, Horton K, et al. Artificial intelligence and echocardiography: a primer for cardiac sonographers. J Am Soc Echocardiogr. 2020;33:1061-6.

[4] Sahashi Y, Ouyang D, Okura H, et al. AI-echocardiography: Current status and future direction. J Cardiol. 2025.

[5] Park J, Yoon YE, Jang Y, et al. Novel deep learning framework for simultaneous assessment of left ventricular mass and longitudinal strain: clinical feasibility and validation in patients with hypertrophic cardiomyopathy. Journal of Echocardiography. 2025:1-12.

[6] Park J, Kim J, Jeon J, et al. Artificial intelligence-enhanced comprehensive assessment of the aortic valve stenosis continuum in echocardiography. EBioMedicine. 2025;112.

[7] Jang Y, Choi H, Yoon YE, et al. An artificial intelligence-based automated echocardiographic analysis: enhancing efficiency and prognostic evaluation in patients with revascularized STEMI. Korean circulation journal. 2024;54:743-56.

[8] Park J, Jeon J, Yoon YE, et al. Artificial intelligence-enhanced automation of left ventricular diastolic assessment: a pilot study for feasibility, diagnostic validation, and outcome prediction. Cardiovascular Diagnosis and Therapy. 2024;14:352.

[9] Long A, Finer J, Hartman H, et al. Deep learning for echocardiographic assessment and risk stratification of aortic, mitral, and tricuspid regurgitation: the DELINEATE-Regurgitation study. Eur Heart J. 2025:ehaf248.

[10] Vrudhula A, Vukadinovic M, Haeffele C, et al. Automated Deep Learning Phenotyping of Tricuspid Regurgitation in Echocardiography. JAMA cardiology. 2025;10:595-602.

[11] Vrudhula A, Duffy G, Vukadinovic M, et al. High-throughput deep learning detection of mitral regurgitation. Circulation. 2024;150:923-33.

[12] Agency NIS. Open AI Dataset Project (AI-Hub). 2024.

[13] Park J, Kim J, Jeon J, et al. Single View Echocardiographic Analysis for Left Ventricular Outflow Tract Obstruction Prediction in Hypertrophic Cardiomyopathy: A Deep Learning Approach. medRxiv. 2025:2025.03. 10.25323713.

[14] Pandian NG, Kim JK, Arias-Godinez JA, et al. Recommendations for the use of echocardiography in the evaluation of rheumatic heart disease: a report from the American Society of Echocardiography. J Am Soc Echocardiogr. 2023;36:3-28.

[15] Mitchell C, Rahko PS, Blauwet LA, et al. Guidelines for performing a comprehensive transthoracic echocardiographic examination in adults: recommendations from the American Society of Echocardiography. J Am Soc Echocardiogr. 2019;32:1-64.

[16] Jeon J, Ha S, Yoon YE, et al. Echocardiographic view classification with integrated out-of-distribution detection for enhanced automatic echocardiographic analysis. arXiv. 2023.

[17] Fan H, Xiong B, Mangalam K, et al. Multiscale vision transformers. Proceedings of the IEEE/CVF international conference on computer vision2021. p. 6824-35.

[18] Knackstedt C, Bekkers SC, Schummers G, et al. Fully automated versus standard tracking of left ventricular ejection fraction and longitudinal strain: the FAST-EFs multicenter study. Journal of the American College of Cardiology. 2015;66:1456-66.

[19] Ouyang D, He B, Ghorbani A, et al. Video-based AI for beat-to-beat assessment of cardiac function. Nature. 2020;580:252-6.

[20] Zhang J, Gajjala S, Agrawal P, et al. Fully automated echocardiogram interpretation in clinical practice: feasibility and diagnostic accuracy. Circulation. 2018;138:1623-35.

[21] Ghorbani A, Ouyang D, Abid A, et al. Deep learning interpretation of echocardiograms. NPJ digital medicine. 2020;3:10.

[22] Strom JB, Playford D, Stewart S, et al. An artificial intelligence algorithm for detection of severe aortic stenosis: a clinical cohort study. JACC: Advances. 2024;3:101176.

[23] Krishna H, Desai K, Slostad B, et al. Fully automated artificial intelligence assessment of aortic stenosis by echocardiography. J Am Soc Echocardiogr. 2023;36:769-77.

[24] Wessler BS, Huang Z, Long Jr GM, et al. Automated detection of aortic stenosis using machine learning. J Am Soc Echocardiogr. 2023;36:411-20.

[25] Holste G, Oikonomou EK, Mortazavi BJ, et al. Severe aortic stenosis detection by deep learning applied to echocardiography. Eur Heart J. 2023;44:4592-604.

[26] Park J, Kim J, Jeon J, et al. Deep Learning–Based Detection and Severity Assessment of Bicuspid Aortic Valve Stenosis. J Am Soc Echocardiogr. 2025.

[27] Holste G, Oikonomou EK, Tokodi M, et al. Complete AI-Enabled Echocardiography Interpretation With Multitask Deep Learning. JAMA. 2025;334:306-18.

[28] Vukadinovic M, Chiu I-M, Tang X, et al. Comprehensive echocardiogram evaluation with view primed vision language AI. Nature. 2025:1-3.

Table 1. Baseline Characteristics

	Developmental Dataset			p-value*	External Test	p-value†
	Training	**Validation**	**Internal Test**			
No. of Patients	**3458**	**429**	**430**		**2254**	
Age, years	55.4 ± 17.3	55.4 ± 17.1	55.3 ± 17.7	0.996	66.6 ± 15.9	<0.001
Male, n (%)	1836 (53.1%)	207 (48.3%)	220 (51.2%)	0.143	1182 (52.4%)	0.665
BMI, kg/m²	23.7 ± 3.6	23.8 ± 3.7	23.8 ± 3.7	0.917	23.6 ± 4.1	0.345
No. of TTE exams	**3485**	**429**	**430**		**2262**	
MS grade, n (%)						
Mild	71 (2.0%)	10 (2.3%)	9 (2.1%)	0.817	21 (0.9%)	0.008
Moderate	144 (4.1%)	19 (4.4%)	14 (3.3%)		147 (6.5%)	
Severe	121 (3.5%)	19 (4.4%)	12 (2.8%)		82 (3.6%)	
MR grade, n (%)						
Mild	201 (5.8%)	25 (5.8%)	25 (5.8%)	0.633	977 (43.2%)	<0.001
Moderate	516 (14.8%)	53 (12.4%)	68 (15.8%)		414 (18.3%)	
Severe	1576 (45.2%)	194 (45.2%)	179 (41.6%)		230 (10.2%)	
Etiology						
Normal	1096 (31.4%)	146 (34.0%)	149 (34.7%)	0.497	542 (24.0%)	<0.001
Rheumatic	386 (11.1%)	47 (11.0%)	36 (8.4%)		269 (11.9%)	
Degenerative	136 (3.9%)	14 (3.3%)	12 (2.8%)		507 (22.4%)	
Prolapse	1195 (34.3%)	142 (33.1%)	141 (32.8%)		308 (13.6%)	
Functional	672 (19.3%)	80 (18.6%)	92 (21.4%)		636 (28.1%)	

p-value* indicates comparisons among the training, validation, and internal test datasets.
p-value† represents comparisons between the internal and the external test datasets.
BMI = body mass index; MR = mitral regurgitation; MS = mitral stenosis

Table 2. Diagnostic Performance of the Proposed Deep Learning Model on Internal and External Test Datasets

	Internal Test Dataset						External Test Dataset					
	Accuracy	**Precision**	**Sensitivity**	**Specificity**	**F1-score**	**AUROC**	**Accuracy**	**Precision**	**Sensitivity**	**Specificity**	**F1-score**	**AUROC**
Normal	0.986	0.967	0.993	0.982	0.980	0.997	0.938	0.800	0.987	0.922	0.884	0.992
Rheumatic	0.970	0.811	0.833	0.982	0.822	0.968	0.966	0.900	0.803	0.988	0.849	0.966
Degenerative	0.981	0.643	0.750	0.988	0.692	0.980	0.885	0.840	0.600	0.967	0.700	0.931
Prolapse	0.951	0.929	0.922	0.965	0.925	0.985	0.942	0.879	0.662	0.986	0.756	0.942
Functional	0.944	0.895	0.837	0.973	0.865	0.969	0.895	0.763	0.910	0.889	0.830	0.957

AUROC = area under the receiver operating characteristic curve

FIGURE LEGENDS

Figure 1. Multi-view Deep Learning Architecture for Mitral Valve Disease Etiology Classification. The model integrates limited routine echocardiographic views using a shared spatiotemporal encoder and view-specific feature projections to infer mitral valve etiology.

Figure 2. Mitral Regurgitation Severity Distribution in Developmental and External Cohorts. Distribution of mitral regurgitation (MR) severity (mild, moderate, and severe) across major etiologic categories in the developmental and external datasets. The external dataset showed a relative shift toward milder MR severity compared with the developmental dataset across several etiologies.

Figure 3. Confusion Matrices of Deep Learning-based Mitral Valve Etiology Classification in the Internal and External Test Datasets.

Figure 4. Representative Examples of Deep Learning-Based Predictions in Cases with Multiple Mitral Valve Etiologies. (A) A woman in her 90s with mixed *functional* and *degenerative* mitral regurgitation (MR). The patient had severe ischemic cardiomyopathy involving multivessel territories with a left ventricular ejection fraction of 29%, resulting in marked leaflet tethering consistent with functional MR. Concomitant mitral annular calcification was also evident, suggesting degenerative changes. The deep learning (DL) model predicted functional mitral valve disease. **(B)** A man in his 80s with coexisting *functional* and *prolapse* mitral valve pathology. Left ventricular ejection fraction was preserved (66%);

however, a regional wall motion abnormality of the mid-posterolateral wall was present, contributing to functional MR. In addition, prolapse of the anterior mitral leaflet was observed on the parasternal long-axis view. The DL model predicted mitral valve prolapse.

Figure 5. Attention Maps Highlighting Anatomically Relevant Regions for Mitral Valve Etiology Classification. Attention maps illustrate regions predominantly weighted by the model across routine echocardiographic views during mitral valve etiology inference.

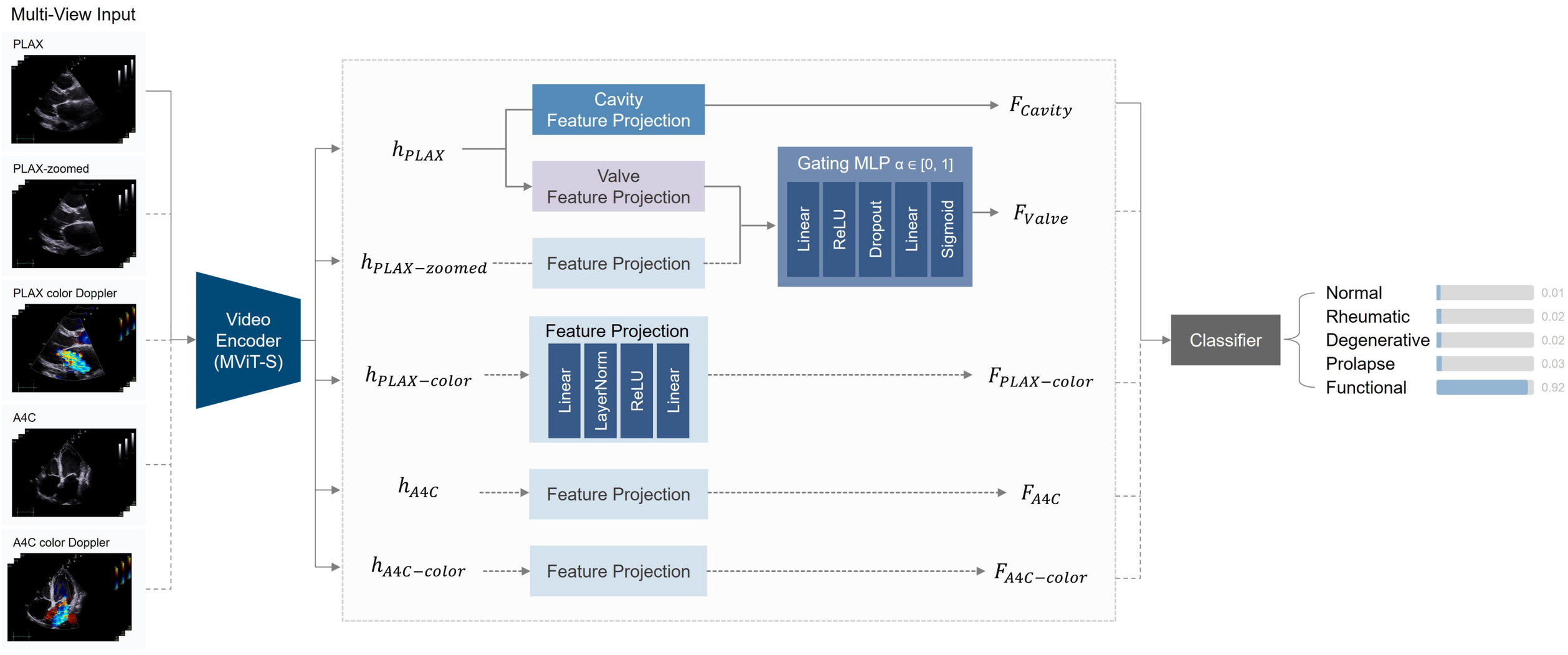
Multi-View Input
PLAX
PLAX-zoomed
PLAX color Doppler
A4C
A4C color Doppler
Video Encoder (MViT-S)
h_{PLAX}
$h_{PLAX-zoomed}$
$h_{PLAX-color}$
h_{A4C}
$h_{A4C-color}$
Cavity Feature Projection
Valve Feature Projection
Feature Projection
Gating MLP α ∈ [0, 1]
Linear
ReLU
Dropout
Linear
Sigmoid
Feature Projection
Linear
LayerNorm
ReLU
Linear
Feature Projection
Feature Projection
F_{Cavity}
F_{Valve}
$F_{PLAX-color}$
F_{A4C}
$F_{A4C-color}$
Classifier
Normal 0.01
Rheumatic 0.02
Degenerative 0.02
Prolapse 0.03
Functional 0.92

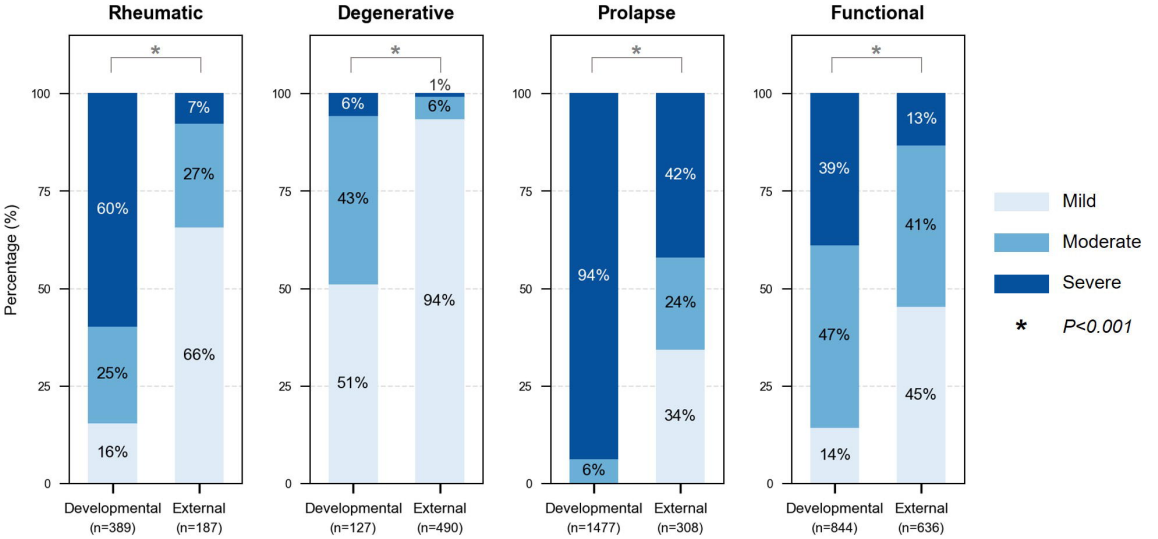
Rheumatic
Degenerative
Prolapse
Functional
Percentage (%)
100
75
50
25
0
*
60%
25%
16%
7%
27%
66%
6%
43%
51%
1%
6%
94%
94%
6%
42%
24%
34%
39%
47%
14%
13%
41%
45%
Developmental
(n=389)
External
(n=187)
Developmental
(n=127)
External
(n=490)
Developmental
(n=1477)
External
(n=308)
Developmental
(n=844)
External
(n=636)
Mild
Moderate
Severe
* P<0.001

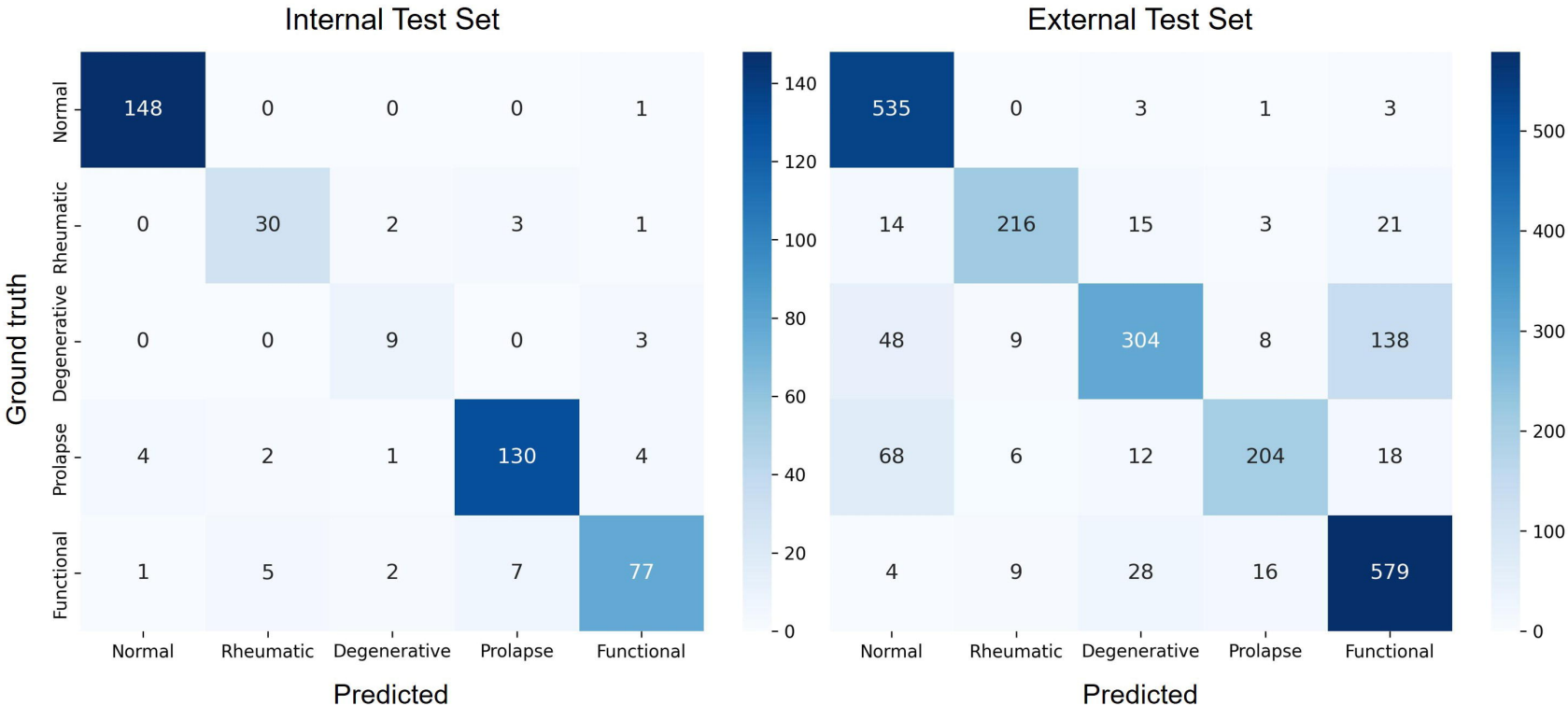
Internal Test Set
External Test Set
Ground truth
Predicted
Normal
Rheumatic
Degenerative
Prolapse
Functional
148 0 0 0 1
0 30 2 3 1
0 0 9 0 3
4 2 1 130 4
1 5 2 7 77
535 0 3 1 3
14 216 15 3 21
48 9 304 8 138
68 6 12 204 18
4 9 28 16 579
0 20 40 60 80 100 120 140
0 100 200 300 400 500

(A)

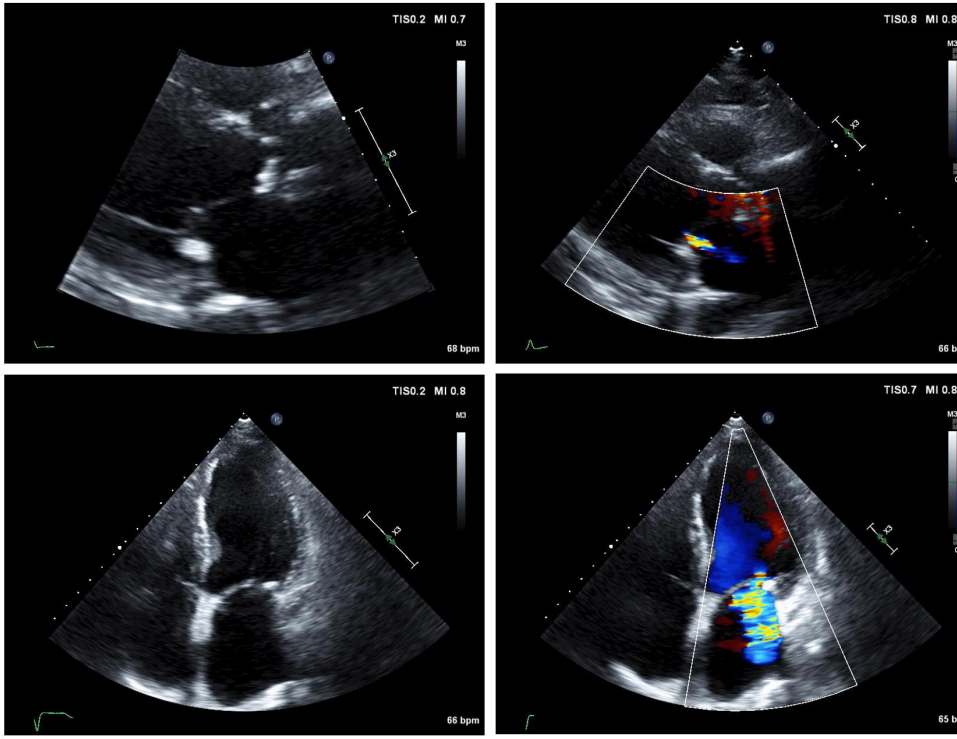
TIS0.2 MI 0.7
M3
68 bpm
TIS0.8 MI 0.8
M3 M4
cm/s
66 bpm
TIS0.2 MI 0.8
M3
66 bpm
TIS0.7 MI 0.8
M3 M4
cm/s
65 bpm

(B)

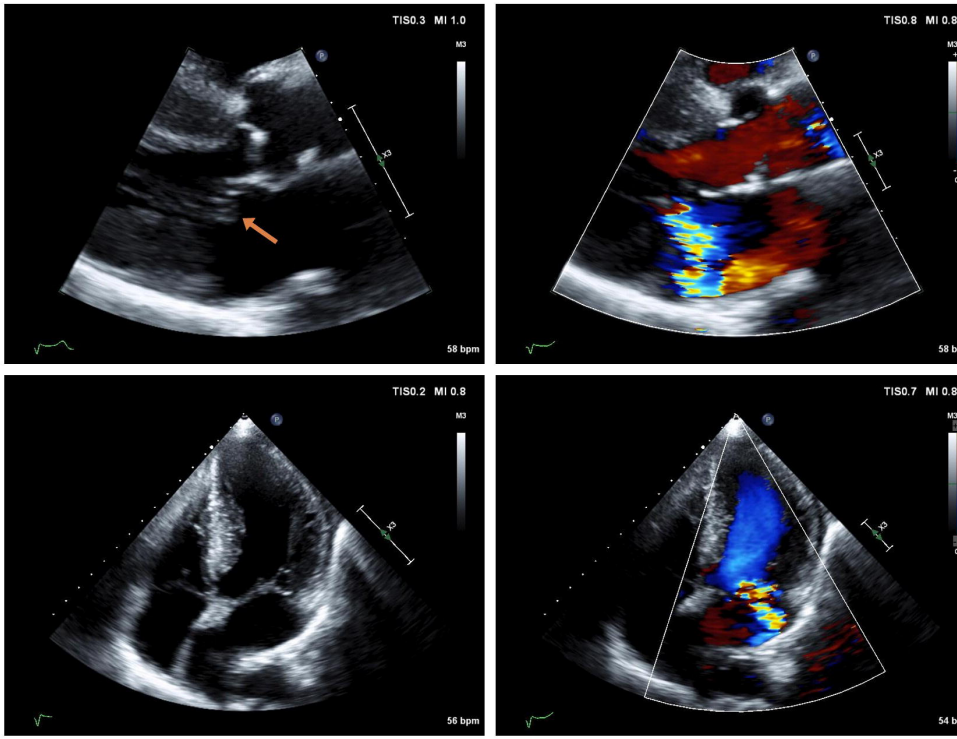
TIS0.3 MI 1.0
M3
58 bpm
TIS0.8 MI 0.8
M3 M4
cm/s
58 bpm
TIS0.2 MI 0.8
M3
56 bpm
TIS0.7 MI 0.8
M3 M4
cm/s
54 bpm

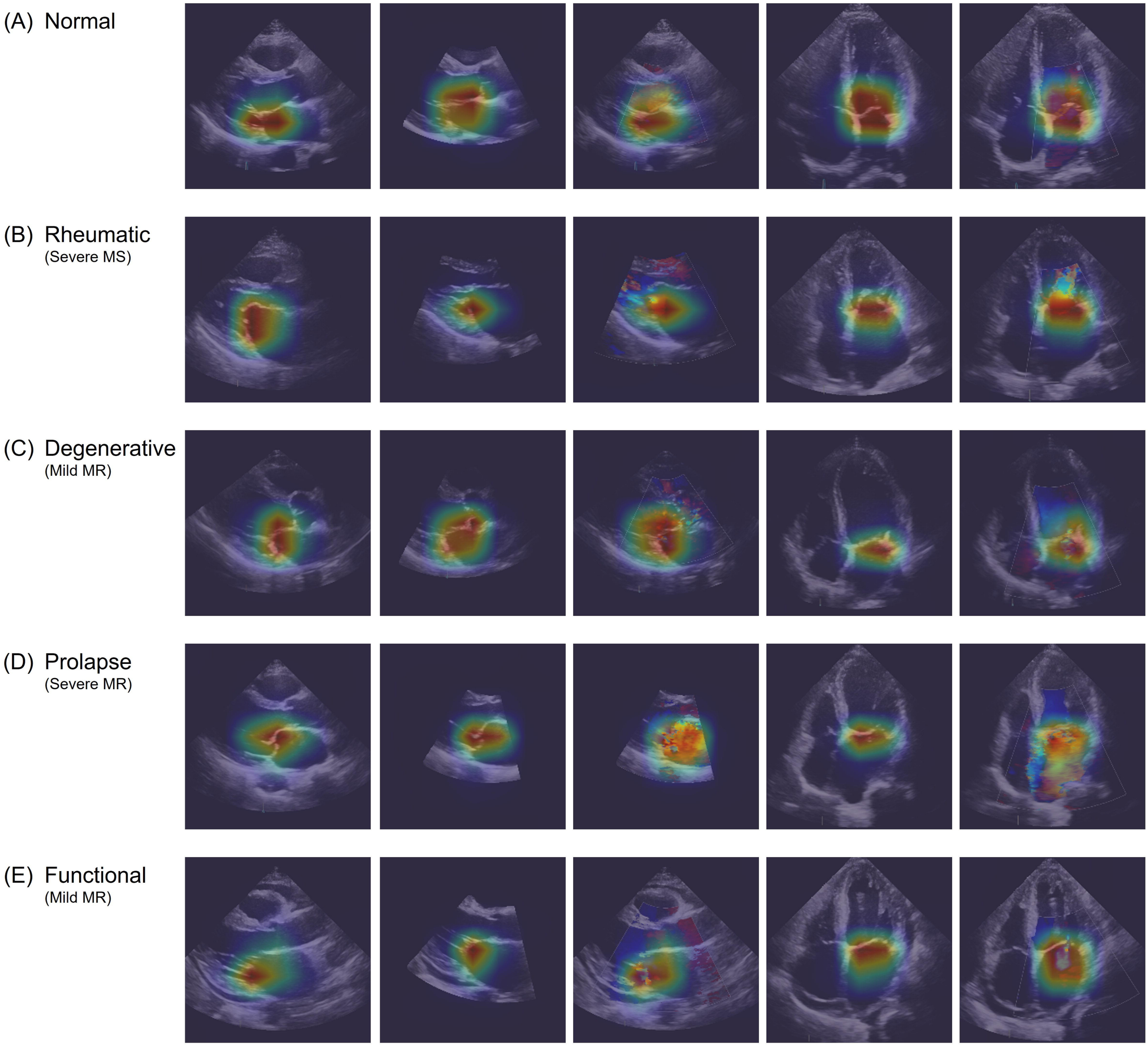
(A) Normal
(B) Rheumatic
(Severe MS)
(C) Degenerative
(Mild MR)
(D) Prolapse
(Severe MR)
(E) Functional
(Mild MR)

Mitral Valve Etiologies Classification Network

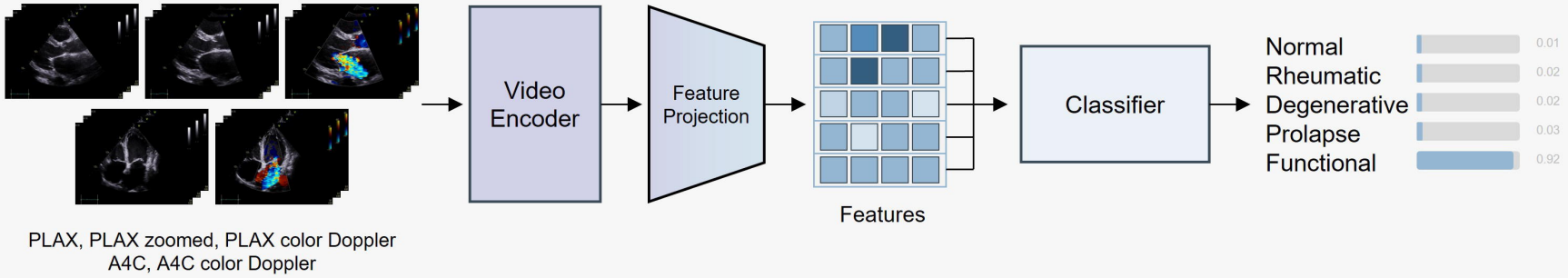

Internal test set (N=430)

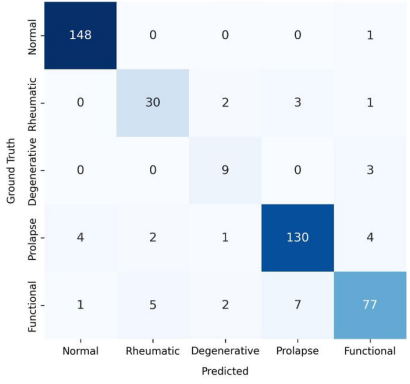

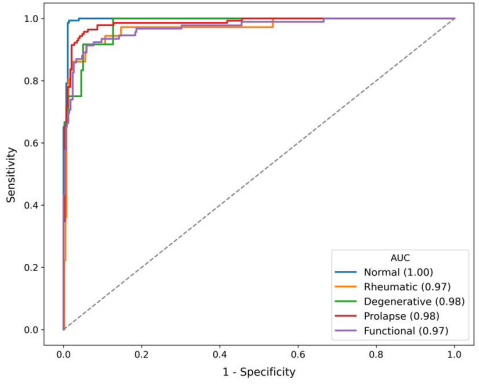
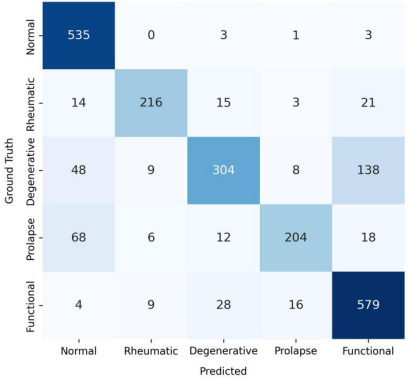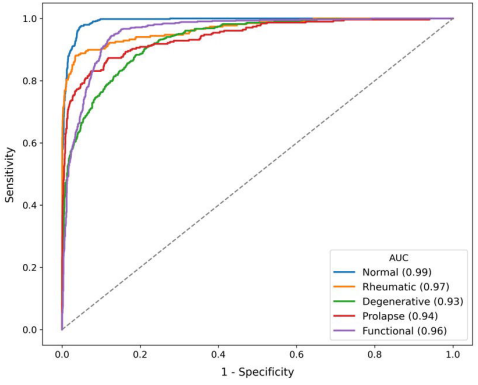
External test set (N=2,262)